A Krylov Model Reduction Methodology for Articulated, Multi-Flexible Body Structures

Allan Y. Lee

Jet Propulsion Laboratory

Abstract

A Krylov model reduction methodology for articulated, multi-flexible body structures is proposed in this research, This methodology generates reduced-order component models without solving any eigenvalue problem. The reduced-order system model obtained with these component models matches exactly a specified number of low-frequency moments of the full-order system. Additionally, all structural modes that contributed significantly to the input-to-output mapping of the full-order system are closely captured by the reduced-order system model, The effectiveness of the proposed methodology in generating reduced-order system models which capture both the time and frequency-domain information of the full-order models, at multiple system configurations, and over a frequency range of interest, has been successfully validated using a finite-element model of the Galileo spacecraft.

Background and Motivation

To simulate and analyze the dynamical motion of an articulated, multi-flexible body structure, one can use multibody simulation packages such as DISCOS.[1] To this end, one must supply appropriate models for all the flexible components involved, For complex systems such as the Galileo spacecraft, practical considerations (e.g., simulation time) impose limits on the number of modes that each flexible body can retain in a given simulation. Reduced-order models of the system's flexible components are hence needed.

Model reduction methodologies arc typically used to reduce a "large" systcm model to onc that is "small" enough to facilitate analysis and control design, yet "rich" enough that it retains the salient features of the original system model. While the literature on model reduction is vast, works that address the model reduction n eeds of articulated, multi-flexible

body structures are sparse, and have only appeared recently.[2-8] Here, what is needed is a way of generating reduced-order component models which when reassembled produce a reduced-order system model that retains the salient features of the input-to-output mapping of the full-order model. The Enhanced Projection and Assembly methodology (EP&A),[7] and the Component Modes Projection and Assembly Model Reduction Methodology (COMPARE)[8] are two effective ways of performing this task.

In the EP&A method, a composite mode set, consisting of "important" system modes from all system configurations of interest, and not just from one particular system configuration, is first selected, It is then augmented with static correction modes before being "projected" onto the component models to generate reduced-order component models. To generate the composite mode set, eigenvalue problems for the full-order system models, at multiple system configurations of interest, must be solved repetitively. This is a drawback of the method because solving large eigenvalue problems can be costly. This difficulty is partially alleviated in the COMPARE methods

The above described model reduction methodologies employed eigen-modes and static correction modes in order to preserve both the static gain and the dominant eigen-modes of the full-order system model in the resultant reduced-order system model, However, with regard to the accuracy of the system time response, there is no proof that the best possible basis for reducing the model size is via the system's eigenvectors. Also, in these methodologies, after a costly computation was made to generate the eigenvectors, only a selected few are actually used while the rest is discarded. This is because the identity of the eigen-mode set that dominates the system's input-to-output mapping is not known till the "whole" eigenvalue problem is solved. Noting these shortcomings, we seek a reduction method that will not require solving any eigenvalue problem, and will generate projection vect ors that will actually be used. To this end, Krylov vectors (to be defined in the sequel) will be used to advant age. The effectiveness of the proposed Krylov model reduction methodology will be established using a finite-element model of the Galileo spacecraft.

A Krylov Model Reduction Methodology

Consider a system with two flexible components. The undamped motion of component A is described by

$$M^A_{pp}\ddot{x}^A_p + K^A_{pp}\,x^A_p = G^A_{pa}u^A_a\,, \qquad y^A_m = H^A_{mp}x^A_p\,. \tag{1}$$

In (l), M^A_{pp} and K^A_{pp} are the mass and stiffness mat rix of component A, respectively. Note that the dimensions of the matrix (or vector) are denoted by its subscripts. For example, the dimension of the coordinate vector x^A_p is p, u^A_a is a $a \times 1$ control vector, and G^A_{pa} is a $p \times a$ control distribution matrix, Likewise, the matrix H^A_{mp} is an output distribution matrix, and y^A_m is an output vector. Similar equations can also be written for component B.

The system equations of motion at a particular articulation angle α may be constructed using these component equations, and enforcing displacement compatibility conditions at the component interface (1/F). To this end, let $P(\alpha) = [P^{A^T}_{pe}(\alpha), P^{B^T}_{qe}(\alpha)]^T$ be a full-rank matrix mapping a minimal system state x^S_e into

$$\begin{bmatrix} x^A_p \\ x^B_q \end{bmatrix} = \begin{bmatrix} P^A_{pe}(\alpha) \\ P^B_{qe}(\alpha) \end{bmatrix} [x^S_e], \tag{2}$$

where x^S_e is a system coordinate (e = p+ q – i). One way to generate the $P(\alpha)$ matrix will be described in the sequel (cf. (20-23)). For ease of notation, the dependencies of the matrices P^A_{pe}, P^B_{qe}, etc. on α are dropped hereafter. Substituting $x^A_p = P^A_{pe} x^S_e$ and $x^B_q = P^B_{qe} x^S_e$ into (1) and the corresponding equations for component B, pre-multiplying the resultant equations by $P^{A^T}_{pe}$ and $P^{B^T}_{qe}$, respectively, and summing the resultant equations give

$$M^S_{ee} \ddot{x}^S_e + K^S_{ee} x^S_e = G^S_{ea} u^S_a, \tag{3}$$

$$y^S_i = H^S_{ie} x^S_e, \tag{4}$$

where $M^S_{ee} = P^{A^T}_{pe} M^A_{pp} P^A_{pe} + P^{B^T}_{qe} M^B_{qq} P^B_{qe}$, $K^S_{ee} = P^{A^T}_{pe} K^A_{pp} P^A_{pe} + P^{B^T}_{qe} K^B_{qq} P^B_{qe}$, $G^S_{ea} = P^{A^T}_{pe} G^A_{pa} + P^{B^T}_{qe} G^B_{qa}$, $H^S_{ie} = [\, P^{A^T}_{pe} H^{A^T}_{mp}, P^{B^T}_{qe} H^{B^T}_{lq} \,]^T$. Here, $y^S_i = [y^{A^T}_m \; y^{B^T}_l]^T$, and $t = m + 1$. To arrive at the equation for G^S_{ea}, we have assumed that $u^A_a = u^B_a = u^S_a$. Otherwise, the term $G^S_{ea} u^S_a$ in (3) should be replaced by $[P^{A^T}_{pe} G^A_{pa}, P^{B^T}_{qe} G^B_{qa}][u^{A^T}_a, u^{B^T}_a]^T$.

Combining the Laplace transforms of (3) and (4) produce a system's input-to-output transfer function T(s). The Taylor series expansion of the magnitude of T(s) about s = O is given by

$$T(s) \triangleq Y(s)/U(s) = \sum_{k=0}^{\infty} (-s^2)^k H^S_{te} (K^{S^{-1}}_{ee} M^S_{ee})^k K^{S^{-1}}_{ee} G^S_{ea} = \sum_{k=0}^{\infty} (-s^2)^k L^k_{ta}. \tag{5}$$

Here, $Y(s)$ and $U(s)$ are the Laplace transforms of y^S_i and u^S_a, respectively, and s $(= j\omega)$ is the Laplace variable. In (5), the t x a matrix $L^k_{ta} \triangleq H^S_{te} (K^{S^{-1}}_{ee} M^S_{ee})^k K^{S^{-1}}_{ee} G^S_{ea}$ is defined

the k^{th} low-frequency moment of the undamped structural system in Refs. 10 and 11. For case of notation, L_{ta}^{k} is denoted by L^{k} hereafter. These low frequency moments can be interpreted using the following identity:

$$L^{k} = \frac{1}{(2k)!} \frac{d^{2k}T(j\omega)}{d\omega^{2k}} \Big|_{\omega=0}, \tag{6}$$

for k = 0,1,2,ss. Hence, *Lo is* the magnitude of the transfer function $T(j\omega)$ at w = O, i.e., the steady state response of the structure due to a unit step input. Similarly, $2L^{1}$ is the second derivative of $T(j\omega)$ with respect to w, evaluated at w = 0. That is, the curvature of the $T(j\omega)$ plot at w = 0.

A system's low frequency moments are sometimes called its time moments. These names come from the fact that L^{k} can be computed as a time-weighted moment of the syst em's impulse response function.[12] If the goal of model reduction is to generate a model that closely captures the time responses of the full-order system model when it is subjected to low frequency excitations ('low' relative to the fundamental frequency of the structure), then, matching the low frequency moments between the full and reduced-order models is an effect ive way.[13] The preservation of other meaningful parameters of the full-order model, such as the high frequency moments (Markov parameters) in the reduced-order model has also been suggested. See, for example, Ref. 13.

To obtain a reduced-order model that matches the first c ($\leq \text{rank}(M_{ee}^{S})$) low frequency moments of the full-order model, consider the following Ritz transformation .

$$x_{e}^{S} = \Pi_{ec}^{S} \eta_{c}^{S}, \tag{7}$$

Here, η_{c}^{S} is a reduced set of generalized coordinates, and Π_{ec}^{S} is a projection matrix, given by[10,11]

$$\Pi_{ec}^{S} = [\Psi_{1}, \ldots, \Psi_{c-1}, K_{ee}^{S^{-1}} H_{te}^{S^{T}}]. \tag{8}$$

The first c-1 vectors in Π_{ec}^{S} are frequently referred to in the literature as Krylov vectors, and they can be generated by a simple Krylov recurrence formula[9,14]

$$\begin{aligned} \Psi_{1} &= K_{ee}^{S^{-1}} G_{ea}^{S}, \\ \Psi_{k+1} &= K_{ee}^{S^{-1}} M_{ee}^{S} \Psi_{k}, \qquad k = 1, \ldots, c-2. \end{aligned} \tag{9}$$

It is clear from (9) that Krylov vectors are characterized by both the material properties of the structure (K_{ee}^S, M_{ee}^S) and the external load distribution vector (G_{ea}^S). In contrast, eigenvectors (used in, e.g., the COMPARE methodology) are just characteristic modes of the structure, independent of the external loading. The above described Krylov algorithm also has an interesting physical interpretation.[14] The first Krylov vector represents the static response of the structure to a given load distribution. The dynamic forces which arc neglected in this static analysis are of the form $\omega_L^2 M_{ee}^S \Psi_1$, where ω_L represents a typical frequency component of the loading. This error vector is then applied in the next step as an 'inertial' load to generate the next Krylov vector.

The inclusion of the last vector $K_{ee}^{S^{-1}} H_{te}^{S^T}$ in (8) can be interpreted as follows. Consider a simplified case with a single input and a single output, i.e., $a = t = 1$ in (3-4). First, wc note that the transfer function from the control input u_a^S to the output y_t^S is identical to that from the input y_t^S to u_a^S. Next, for the later transfer function, the control and output distribution matrices are $H_{te}^{S^T}$ and $G_{ea}^{S^T}$, respectively. Hence the term $K_{ee}^{S^{-1}} H_{te}^{S^T}$ in (8) is also a 'static response' term, to be included in the projection matrix.

The reduced-order system model obtained using Π_{ec}^S is given by

$$M_{cc}^S \ddot{\eta}_c^S + K_{cc}^S \eta_c^S = G_{ca}^S u_a^S, \tag{lo}$$

$$y_t^S = H_{tc}^S \eta_c^S, \tag{11}$$

where $M_{cc}^S = \Pi_{ec}^{S^T} M_{ee}^S \Pi_{ec}^S$, $K_{cc}^S = \Pi_{ec}^{S^T} K_{ee}^S \Pi_{ec}^S$, $G_{ca}^S = \Pi_{ec}^{S^T} G_{ea}^S$, and $H_{tc}^S = H_{te}^S \Pi_{ec}^S$. The proof that the first c low frequency moments of the reduced-order model (cf. (10-11)) are identical to those of the full-order model (cf. (3-4)) is given in Refs. 10 and 11. However, note that (3-4) as well as (10-11) represent undamped system dynamics. It was found in Ref. 10 that when these undamped Krylov vectors are used to reduce a damped system model, the resultant reduced-order model no longer possesses the parameter-matching property. On the other hand, since the damping levels of most spacecraft structures are typically very low (below 0.25%), the error involved when these unclamped Krylov vectors are applied on lightly damped structures should be minimal.

A Krylov Model Reduction Methodology for Articulated, Multi-flexible Body Structures

Let $(\Phi_{cc}^S, \Lambda_{cc}^S) = \text{eig}(K_{cc}^S, M_{cc}^S)$. The "modal" equivalence of (10-11) is

$$I_{cc}^S \ddot{\phi}_c^S + \Lambda_{cc}^S \phi_c^S = \Phi_{cc}^{S^T} G_{ca}^S u_a^S, \tag{12}$$

$$y_t^S = H_{tc}^S \Phi_{cc}^S \phi_c^S . \tag{13}$$

Here, ϕ_c^S is the modal coordinate ($\eta_c^S = \Phi_{cc}^S \phi_c^S$), $\Phi_{cc}^{S^T} M_{cc}^S \Phi_{cc}^S = I_{cc}^S$, and $\Lambda_{cc}^S = \Phi_{cc}^{S^T} K_{cc}^S \Phi_{cc}^S$ contains the undamped eigenvalues of the Krylov model along its diagonal. Typically, c is much smaller than e, Hence, the numerical effort involved in solving this eigenvalue problem is trivial compared to that involved in solving the original e x e eigenvalue problem.

Not all the modes in Λ_{cc}^S contributed significantly to the system's input-to-output mapping. In the proposed method, only b of the c modes are kept while the remaining d ($= c - d$) modes are discarded. Ways to select important system's modes that make significant contribution to the system's input-to-output mapping have been suggested.[15,16] In our study, we use the Modal Influence Coefficient (MIC) defined in Ref. 7 to rank the relative importance of the system's Krylov modes.

For articulated, multi-flexible bodies structures, a set of "important" Krylov modes at a particular system configuration might be different from those of other configurations. Hence, wc need to decide on a system configuration α_G at which the selected set of '(important" modes encompasses important modes from, all system configurations, The determination of α_G will be illustrated by an example in the sequel. With this understanding, we have

$$\eta_c^S = \Phi_{cc}^S \phi_c^S = \begin{bmatrix} \Phi_{cb}^S & \Phi_{cd}^S \end{bmatrix} \begin{bmatrix} \phi_b^S \\ \phi_d^S \end{bmatrix} \doteq \Phi_{cb}^S \phi_b^S , \tag{14}$$

where ϕ_b^S and ϕ_d^S are the "kept" and '{discarded" coordinates, respectively. Before the kept mode set Φ_{cb}^S is projected onto the component models, it has to be augmented with a static correction mode(s). This is the same augmentation step that was employed in both the EP&A and COMPARE methodologies.[6-8] To this end, the system modal equation (12-13) is decomposed into its kept and discarded parts:

$$I_{bb} \ddot{\phi}_b^S + \Lambda_{bb}^S \phi_b^S = \Phi_{cb}^{S^T} G_{ca}^S u_a^S , \tag{15}$$

$$I_{dd} \ddot{\phi}_d^S + \Lambda_{dd}^S \phi_d^S = \Phi_{cd}^{S^T} G_{ca}^S u_a^S . \tag{16}$$

The static contribution of the discarded mode set Φ_{cd}^S can be approximated by a smaller mode Set Φ_{ca}^S, To find Φ_{ca}^S, consider the following Ritz transformation

$$\phi_d^S = R_{da}^S \phi_a^S \triangleq [\Lambda_{dd}^{S^{-1}} \Phi_{cd}^{S^T} G_{ca}^S] \phi_a^S . \tag{17}$$

Here ϕ_a^S is the generalized coordinate associated with the augmented mode set Φ_{ca}^S. It can be shown that the static gain of the original system (cf. (12-13)) is exactly captured by a reduced-order system model obtained using the mode set $[\Phi_{cb}^S \Phi_{ca}^S] = [\Phi_{cb}^S \Phi_{cd}^S R_{da}^S]$.[6]

The augmented, statically complete mode set $[\Phi_{cb}^S \Phi_{ca}^S]$ can now be projected onto the component models: $x_p^A \doteq P_{pe}^A \Pi_{ec}^S [\Phi_{cb}^S \Phi_{ca}^S] \phi_v^A \triangleq \Psi_{pv}^A \phi_v^A$. Here, $v = b + a$, and ϕ_v^A denotes a reduced set of generalized coordinates of component A. The substitution of the last relation into (1) produces the '{constrained') equations of motion for component A:

$$\Psi_{pv}^{A^T} \Psi_{pv}^A \ddot{\phi}_v^A + \Psi_{pv}^{A^T} \Lambda_{pp}^A \Psi_{pv}^A \phi_v^A = \Psi_{pv}^{A^T} G_{pa}^A u_a^A , \tag{18}$$

$$\Psi_{qv}^{B^T} \Psi_{qv}^B \ddot{\phi}_v^B + \Psi_{qv}^{B^T} \Lambda_{qq}^B \Psi_{qv}^B \phi_v^B = \Psi_{qv}^{B^T} G_{qa}^B u_a^B . \tag{19}$$

A similar equation for component B is given in (19),

A reduced-order system model can now be generated using (18-19), and the I/F compatibility relations. The I/F relation is given by $C_{ip}^A x_p^A + C_{iq}^B x_q^B = O_i$, where C_{ip}^A and C_{iq}^B arc matrices that establish the constraint relations between the component models, and i is the number of constraint relations. In terms of the reduced coordinates of component A and B, wc have

$$[C_{ip}^A \Psi_{pv}^A C_{iq}^B \Psi_{qv}^B] \begin{bmatrix} \phi_v^A \\ \phi_v^B \end{bmatrix} \triangleq [D_{in}] \begin{bmatrix} \phi_v^A \\ \phi_v^B \end{bmatrix} \doteq 0 , \tag{20}$$

where n = 2v. To construct the reduced-order system model, we partition the "compatibility" matrix D_{in} using the SVD technique

$$[D_{in}] = [U_{ii}] [\Sigma_{ii} , O_{ih}] \begin{bmatrix} P_{ni}^T \\ P_{nh}^T \end{bmatrix} , \tag{21}$$

where $h = n - i$, Σ_{ii} is an i x i diagonal matrix with the i singular values of the matrix D_{in} along its diagonal, and O_{ih} is an i x h null matrix. The partitioned matrix P_{nh} in (22) can be used as follows[3,6,7]

$$\begin{bmatrix} \phi_v^A \\ \phi_v^B \end{bmatrix} = [P_{nh}] \phi_h^S \triangleq \begin{bmatrix} P_{vh}^A \\ P_{vh}^B \end{bmatrix} \phi_h^S , \tag{22}$$

where ϕ_h^S denotes the generalized coordinates of a Krylov reduced-order system model. Substituting $\phi_v^A = P_{vh}^A \phi_h^S$ and $\phi_v^B = P_{vh}^B \phi_h^S$ into (18-19), pre-multiplying the resultant equations by $P_{vh}^{A^T}$ and $P_{vh}^{B^T}$, respectively, and summing the resultant equations give

$$M_{hh}^S \ddot{\phi}_h^S + K_{hh}^S \phi_h^S = G_{ha}^S u_a^S , \tag{23}$$

$$y_t^S = H_{th}^S \phi_h^S , \tag{24}$$

where $M^S_{hh} = P^{A^T}_{vh} \Psi^A_{pv} \Psi^A_{pv} P^A_{vh} + P^{B^T}_{vh} \Psi^B_{qv} P^B_{vh}$. Similar expressions can also be written for K^S_{hh}, G^S_{ha}, and H^S_{th}. The steps involved in the Krylov model reduction methodology are illustrated in Fig. 1.

As is apparent from the above described steps, the Krylov model reduction methodology does not involve the solving of any eigenvalue problem (except for a %-nail" one used in the determination of the MICs. Sce (12-13)). Using the statically complete projection matrix $[\Phi^S_{cb} \Phi^S_{ca}]$, the low frequency moments of the full-order system model (cf. (3-4)) are also exactly captured by the reassembled Krylov reduced-order system model (cf. (23-24)), Additionally, all structural modes that contributed significantly to the input-to-output mapping of the full-order system are closely captured by the Krylov models, at all system configurate ions of interest. The effectiveness of this approach will be validated using a finite-element model of the Galileo spacecraft.

Applying the Krylov Model Reduction Methodology on A 28-dof Galileo Model

The effectiveness of the Krylov vectors-based model reduction methodology is evaluated using a 28-dof finite-element model of the Galileo spacecraft.[6] The model, pictured in Fig. 2, is meant to resemble the Galileo spacecraft in its overall features. The spacecraft comprises a 12-clef stator (component A) and a 21-dof rotor (component B). The rotor may be rotated with respect to the stator, at 3.15 rpm, using a spin bearing actuator located at their interface (cf. *Al-131* in Fig. 2). The relative orientation of the rotor with respect to the stator is denoted by the clock angle α, also shown in Fig. 2.

'l'he equations of motion of the spacecraft at any clock angle α, may be determined using the equations of motion of both the rotor and the stator, and the interface compatibility conditions

$$\begin{bmatrix} x \\ y \\ z \\ \theta_x \\ \theta_y \end{bmatrix}_{A_1} = \begin{bmatrix} \cos\alpha & \sin\alpha & 0 & 0 & 0 \\ -\sin\alpha & \cos\alpha & 0 & 0 & 0 \\ 0 & 0 & 1 & 0 & 0 \\ 0 & 0 & 0 & \cos\alpha & \sin\alpha \\ 0 & 0 & 0 & -\sin\alpha & \cos\alpha \end{bmatrix} \begin{bmatrix} x \\ y \\ z \\ \theta_x \\ \theta_y \end{bmatrix}_{B_1} \quad (25)$$

The resultant system model has seven rigid-body modes and 21 flexible modes. The natural frequencies of rotor, stator, and the system (at α = 0°) are tabulated in Table 1. As α changes, some system frequencies increase, others decrease, while a few remain unchange.

For the purpose of controller design, reduced-order systcm models at all configurations of interest arc needed. Let us use the Krylov methodology to perform this task. Upon the removal of the seven rigid-body modes, the remaining 21-dof flexible model is reduced using

10 Krylov vectors (i.e., c = 10 in (12-13)). That is, wc are interesting in capturing the top ten low frequency moments of the full-order system. The MICS (normalized by the largest MIC) of these Krylov modes in the reduced-order model are tabulated in Table 2, from which we conclude that only four modes (modes 2, 3, 4, and 5) contributed significantly to the input-to-output mapping. We would have reached the same conclusion have we used a different c.

Table 1 Natural Frequencies of the Full-order Component and System Models (α = 0°)

Mode	Ω_{rotor} (Hz)	Ω_{stator} (Hz)	Ω_{system} (HZ)
1-6	0	0	0
7	*0.1221*	*57.253*	*0*
8	*1.0579*	*57.455*	*0.1106*
9	*2,8638*	*225.24*	*1.0521*
10	*3.4223*	*225.31*	*1.9403*
11	4.9894	1217.7	2,3975
12	5.2217	1404.7	2.8446
13	73.425		3.4648
14	75.821		4.9930
15	76.998		5.4793
16	116.50		6.8081
17	116.51		9.2953
18	994.70		56.060
1 9	994.70		73.429
20	2108.5		75.823
21	2431.9		76.999
22			144.69
23			144.73
24			712.64
25			712.65
26			1217.7
27			1985.9
28			2108.5

Table 2 Normalized MICS of the Krylov Model's Modes (α = 0°, c = 10)

Mode	Ω_{Krylov} (Hz)	MIC	Mode	Ω_{Krylov} (Hz)	MIC
1	0.1106	0.0000	6	9.2953	0.0153
2*	1.0521	0.4305	7	46.199	0.0000
3*	2.3975	1.0000	8	14466	0.0000
4*	4.9930	0.6039	9	1204.9	0.0000
5*	5.4793	0.2524	10	1989.7	0.0000

* Kept Krylov modes

The question now is whether the system's input-to-output mappings at other configurations can also be adequately captured by this 4-mode mode set ? To answer that question, we repeat the MIC calculation at another configuration, with α = 60°. The corresponding normalized MICS are given in Table 3. A comparison of results given in Tables 2 and 3 indicate the followings :

(a) The Krylov modes' frequencies Ω_{Krylov} at α = 60° differ slightly from those obtained at α = O°. For example, the first flexible mode frequency increases slightly from 0.1106 to 0.1123 Hz as α varies from O to 60°.

(b) Whereas 4 modes practically captured the input-to-output mapping of the full-order system at α = 0°, six modes are needed at a system configuration with α = 60°,

Table 3 Normalized MICS of the Krylov Model's Modes (α = 60°)

Mode	Ω_{Krylov} (Hz)	MIC	Mode	Ω_{Krylov} (Hz)	MIC
1*	0.1123	0.1196	6	3.5947	0.0820
2*	1.0520	0.2665	7	4.9689	1.0000
3*	1.8163	0.1149	8*	5.1389	0.7427
4*	2,4863	0,4082	9	7.1271	0.0054
5	2.8750	0.0343	10	9.2079	0.0100

* Kept Krylov modes

Based upon these results, we decide on α_G = 60° as the configuration to perform the Krylov reduction and projections, However, it should be emphasized that other selections, such as α_G = 45 or 72° can also be made, producing results similar to those to be given in the sequel.

Accordingly, we will keep six Krylov modes (mode number 1-4, and 7-8 in Table 3) in the projection mode set, and replace the remaining modes (mode number 5, 6, 9, and 10) with a static correction mode determined using (15-17). Its frequency, at 3.5939 Hz, is rather c1osc to the frequency of mode 6 (3,5947 Hz) in Table 3, which has the highest MIC among the four discarded modes. However, it should be emphasized that the approach suggested by (15-17) should be followed instead of, e.g., projecting the top seven highest MIC modes in Table 3. Results obtained using the latter approach, not given here, show poorer matchings in both the input-to-output frequency responses as well as the low frequency moments.

The selected mode set (with 7 rigid-body and 6+1 flexible modes) is then projected on both the rotor and st ator models. The resultant projected rotor and st ator models, together with the reduced-order system model constructed at $\alpha = 60°$, have 13, 10, ant] 18 degrees of freedom, respectively. Natural frequencies of these component and system models are tabulated in Table 4. Note that the six most dominant modes of the full-order system have been closely captured by the Krylov reduced-order model (to within 0.17%). Bode plot comparisons of the full-order and Krylov reduced-order system models, at various clock angles are depicted in Fig. 3. Here, the actuator input is a negative and a positive torque τ_e about the Z-axis of the rotor and the stator, respectively. The output is a rotation about the Y-axis passing through Point *A*. on the stator (cf. Fig. 2). In these Bode plots, a uniform damping ratio of 0.25% was assumed for both the full and reduced-order models. In spite of the fact that no eigenvalue problem was solved in generating these Krylov models, they approximate the frequency responses of the full-order models, at mult iple s ystem configurate ions and over a frequency range of interest.

To compare the low frequency moments (L^k) of the full ancl reduced-order models, we tabulate the values of full-order models' $L^k, k = O,1,...,9$, at six clock angles in Table 5. Note that, the magnitudes of L^k, $k = 3,...,9$, at $\alpha = 0°$, are practically zero. The ratios between these full-order models' L^k and their Krylov reduced-order models' counterparts, $L^k_{\text{Full}}/L^k_{\text{Reduced}}$, are tabulated in Table 6. Clearly, the top ten low frequency moments of the full-order models, at various system configurations of interest, have been captured exactly by the corresponding Krylov models. These results, and those depicted in Fig. 3, clearly establish the effectiveness of the proposed Krylov model reduction methodology in preserving both the time and frequency-clomain information of the full-order model,

Table 4 Natural Frequencies of the Projected Component Models and the Reduced-order System Model (α = 60°) [Krylov Methodology]

Mode	Ω_{system} (Hz)	ω_{rotor} (Hz)	ω_{stator} (Hz)	ω_{system} (Hz)
1-6	0	0	0	0
7	0	0.1221	57.254	0
8	0.1123†	1.0579	57.461	0.1123‡
9	1.0520†	3.2387	225.25	1.0520‡
10	1.8163†	4.9895	226.74	1.8194‡
11	2.4863†	5.2234		2.4872‡
12	2.8750	29.578		3.4041
13	3.5946	116.65		4.9680‡
14	4.9689†			5.1358‡
15	5.1388†			7.1554
16	7.1262			9.1837
17	9.2069			51.280
18	56.060			145.95
19	73.429			
20	75.823			
21	76.999			
22	144.69			
23	144.73			
24	712.64			
25	712.64			
26	1217.7			
27	1985.9			
28	2108.5			

† Dominant full-order system modes (α = 600). See also Table 3.

‡ Dominant full-order modes closely captured by the Krylov model (α = 600).

Table 5 Low Frequency Moments (L^k) of the Full-order Models

L^k	0°	15°	30°	45°	60°	72[a]
L^0 x 10-[7]	-1.8910	-1.8009	-1.5520	-1,1973	-0.7973	-0.4?39
L^1 x 10-[8]	-0.2396	0.4015	1.8967	3.2367	3.4613	2.5805
L^2 x 1 0[-8]	*-0.0042*	*1.3059*	*4.3198*	*6.9248*	*7.2071*	*5.3085*
L^3 x 1 0[-7]	-0.0000	*0.2705*	*0.8863*	*1.4057*	*1.4478*	*1.0595*
$L^4 \times 10^{-7}$	-0.0000	*0.5587*	*1.8169*	*2,8524*	*2.9075*	*2,1140*
L^5 x 10^{-7}	-0.0000	1.1539	3.7246	5.7878	5.8389	4.2182
L^6 x 10^{-6}	-0.0000	*0.2383*	*0.7635*	*1.1744*	*1.1726*	*0.8417*
L^7 x 10^{-6}	-0.0000	*0.4922*	*1,5652*	*2.3830*	*2.3548*	*1.6794*
La x10^{-6}	-0.0000	1,0164	3.2086	4.8353	4.7290	3.3509
L^9 x 10-[6]	-0.0000	2.0992	6.5775	9.8113	9.4968	6.6861

Table 6 Ratios of Full to Reduced Models' Low Frequency Moments, $L^k_{\text{Full}}/L^k_{\text{Reduced}}$

k	α = 0°†	*15°*	*30°*	*45°*	*60°*	*72°*
0	1.0000	1.0000	1.0000	1.0000	1.0000	1.0000
1	1.0000	1.0000	1.0000	1.0000	1.0000	1.0000
2	1.0000	1,0000	1.0000	1.0000	1.0000	1.0000
3	–	*1.0000*	*1.0000*	1.0000	*1.0000*	1.0000
4	–	*1,0000*	1.0000	1.0000	1$0000	1.0000
5	–	1,0000	1.0000	1.0000	1.0000	1,0000
6	–	1.0000	1.0000	1.0000	1.0000	1.0000
7		*1.0000*	1,0000	1.0000	1.0000	1.0000
8	–	1.0000	1.0000	1.0000	1.0000	1.0000
9	-	1.0000	1.0000	1.0000	1.0000	1.0000

† Both L^k_{Full} and L^k_{Reduced} + O for k = *3,...,9*. Hence, $L^k_{\text{Full}}/L^k_{\text{Reduced}}$, k = *3,...,9* are undefined.

Concluding Remarks

Eigenvalues and eigenvectors have a definite value in aiding us in our understanding of the dynamic behavior of structures. However, the use of exact eigenvectors as the basis for performing model reduction can be computational costly, and has not been proven to be the best possible approach, A Krylov vectors-based model reduction methodology which dots not require solving any eigenvalue problem is proposed here.

Unlike eigenvectors, Krylov vectors can be easily, and reliably generated using rather

simple algorithm(s). Since Krylov vectors are functions of the spatial distribution of the external loading, different Krylov vectors must be generated for different load distributions. However, this is not a difficult task! Krylov-generated reduced-order component models, when reassembled, produce a reduced-order system model that matches a specified number of low frequency moments of the full-order system model. Additionally, dominant system modes' frequencies are also closely captured. The effectiveness of the Krylov methodology in preserving both the time and frequency-domain information of the full-order model, at multiple system configurations and over a frequency range of interest, has been successfully validated using a G alileo model.

Since the reduced-order models will ultimately be used for nonlinear simulations, the final comparison between the full and reduced-order models should be done in the time domain, However, judging by the fact that the reduced-order system models c1osc1 y reproduced the frequency responses of their full-order counterparts at the various system configurations, we expect to obtain good time-domain results with this approach if the articulation rate is "sufficiently" slow. However, this must be confirmed and quantified via careful nonlinear, time simulations. The effects that increasing slew rate has on the effectiveness of the methodology is an interesting topic to pursue in the future. Other related research topics include: (i) to investigate the possible removals of high frequency extraneous modes using the methodology proposed in Ref. 6; and (ii) to assess the merits/demerits of using the damped Krylov vectors[10] (instead of the undamped Krylov vectors) to reduce the models of lightly clamped structures.

References

1. Bodley, C. S., Devers, A. D., Park, A. C., and Frisch, H. P., "A Digital Computer Program for the Dynamic Interaction Simulation of Controls and Structure (DISCOS)," NASA Technical Paper 1219, Vols. I and II, NASA Center for Aerospace Information, Baltimore, Maryland, May, 1978.
2. Spanos, J.T. and Tsuha, W., "Selection of Component Modes for the Simulation of Flexible Multibody Spacecraft," Journal of Guidance, Navigation, and Control, Vol. 14, No. 2, pp. 278-286, March/April, 1991.
3. Bernard, D., "Projection and Assembly Method for Multibody Component Model Reduction," Journal of Guidance, Control, and Dynamics, Vol. 13, No. 5, Septcnl-

ber/October, 1990.

4. Eke, F.O. and Man, G.K., "Model Reduction in the Simulation of Interconnected Flexible Bodies," Paper AAS S7-455, Proceedings of the AAS/AIAA Astrodynarnics Specialist Conference, Kalispell, Montana, August, 1987.
5. Tsuha, W. and Spanos, J. T., "Reduced Order Component Modes for Flexible Multibody Dynamics Simulations," AIAA Paper 90-662, Proceedings of the AIAA Aerospace Sciences Meeting, Reno, Nevada, January, 1990.
6. Lee, A.Y. "A COMPACT Model Reduction Methodology for Articulated, Multi-flexible Body Structures," Paper 93-3709, Proceedings of the AIAA Guidance, Navigation, and Control Conference, Monterey, August 9-11, 1993.
7. Lee, A.Y. and Tsuha, W. S., "An Enhanced Projection and Assembly Model Reduction Methodology," Journal of Guidance, Control, and Dynamics, Vol. 17, No. 1, pps. 69-75, January/February, 1994.
8. Lee, A.Y. and Tsuha, W. S., "A Component Model Reduction Methodology for Articulated Flexible Structures ," Journal of Guidance, Control, and Dynamics, (to appear).
9. Craig, R, R., Jr., Structural Dynamics: An Introduction to Computer Methods, John Wiley and Sons, Inc., New York, 1981.
10. Su, T.Z. and Craig, R.R.,Jr.,"Model Reduction and Control of Flexible Structures Using Krylov Vectors," Journal of Guidance, Control, and Dynamics, Vol. 14, No. 2, pps. 260-267, March/April, 1991.
11. Su, T.Z. and Craig, R. R.,Jr.,"Krylov Model Reduction Algorithm for Undamped Structural Dynamics Systems," Journal of Guidance, Control, and Dynamics, Vol. 14, No. 6, pps. 1311-1313, November/December, 1991.
12. Kailath, T. , Linear Systems, Prentice-Hall, Inc., Englewood Cliff, N. J., 1980.
13. Villemagne, C. and Skelton, R. E., "Model Reduction Using A Projection Formulation," International Journal of Control, Vol. 46, No, 6, pps. 2141-2169, 1987.
14. Wilson, E. L., Yuan, M., and Dickens, J. M., "Dynamic Analysis by Direct Superposition of Ritz Vectors," Earthquake Engineering and Structural Dynamics, Vol. 10, pps. 813-821, 1982.
15. Skelton, R. E., Singh, R., and Ramakrishnan, J., "Component Model Reduction by Component Cost Analysis," AIAA Paper 88-4086, August, 1988.
16. Moore, B, Co, "Principal Component Analysis in Linear Systems : Controllability, Observability, and Model Reduction," IEEE Transaction on Automatic Control, Vol. AC-26, INO. 2, 19s1, pp. 17-32.

Acknowledgments

The research described in this paper was conducted at the Jet Propulsion Laboratory, California Institute of Technology, under a contract with the National Aeronautics and Space Administration. The author wishes to thank his colleagues at JPL, including Dr. W. Gawronski, Dr. F. Hadaegh, Dr. G. Man, and Mr. W. Tsuha for many helpful discussions,

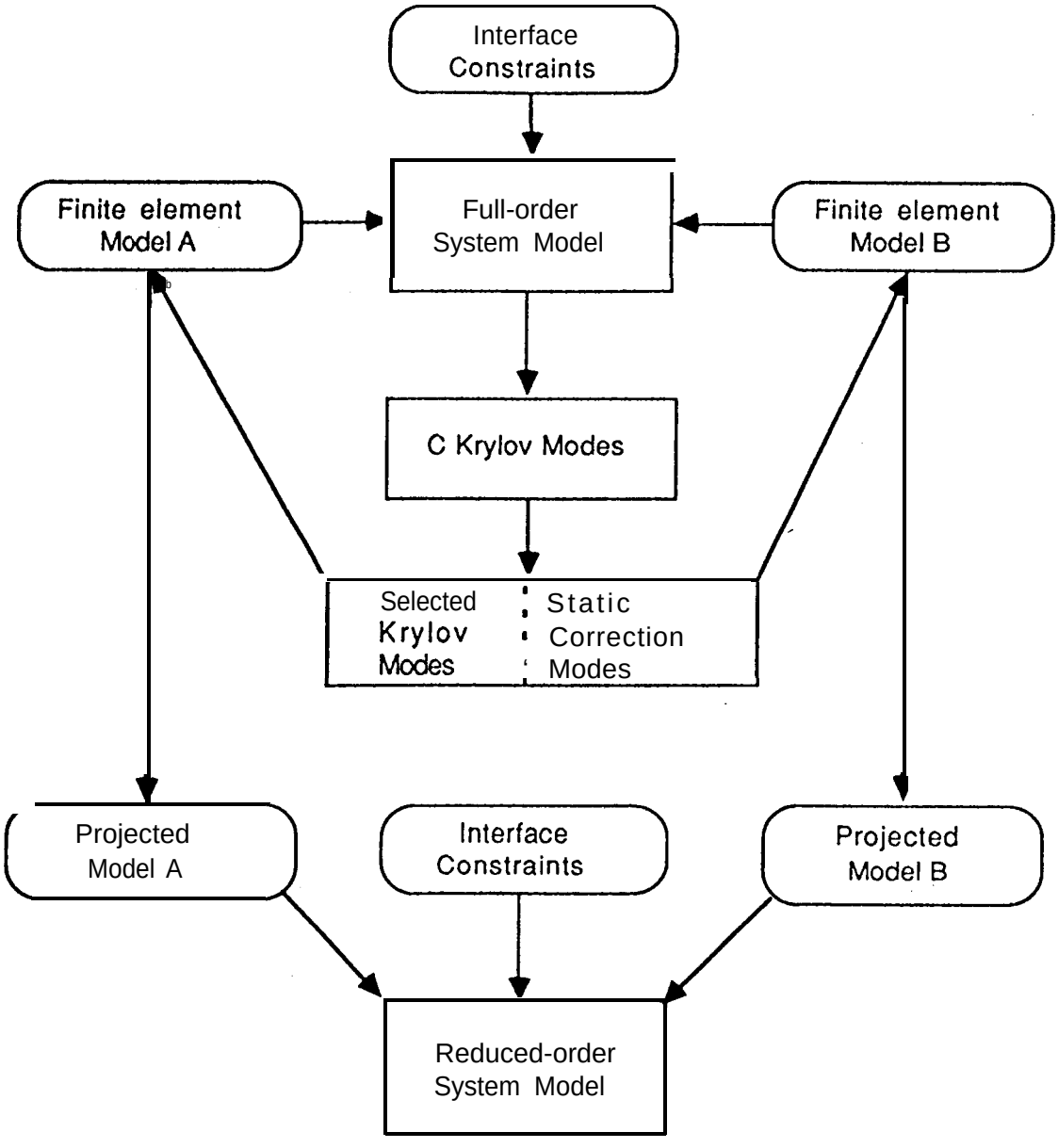

Fig. 1 A Graphical Illustration of the **Krylov** Methodology

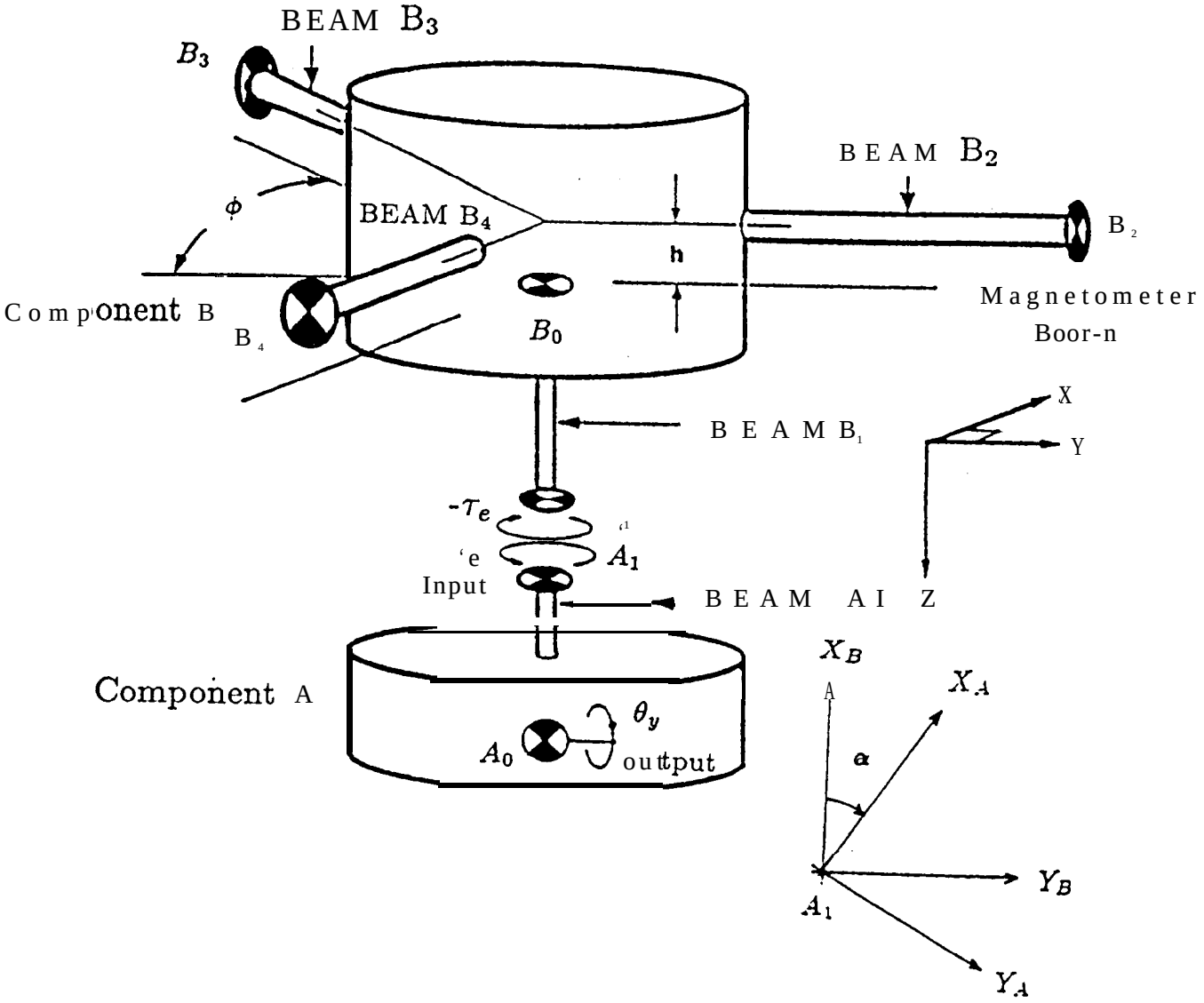

Figure 2 Schematic Diagram of.4 28-dof Galileo Model

Fig, 3 Bode Plot Comparisons of Full and Reduced-order Models

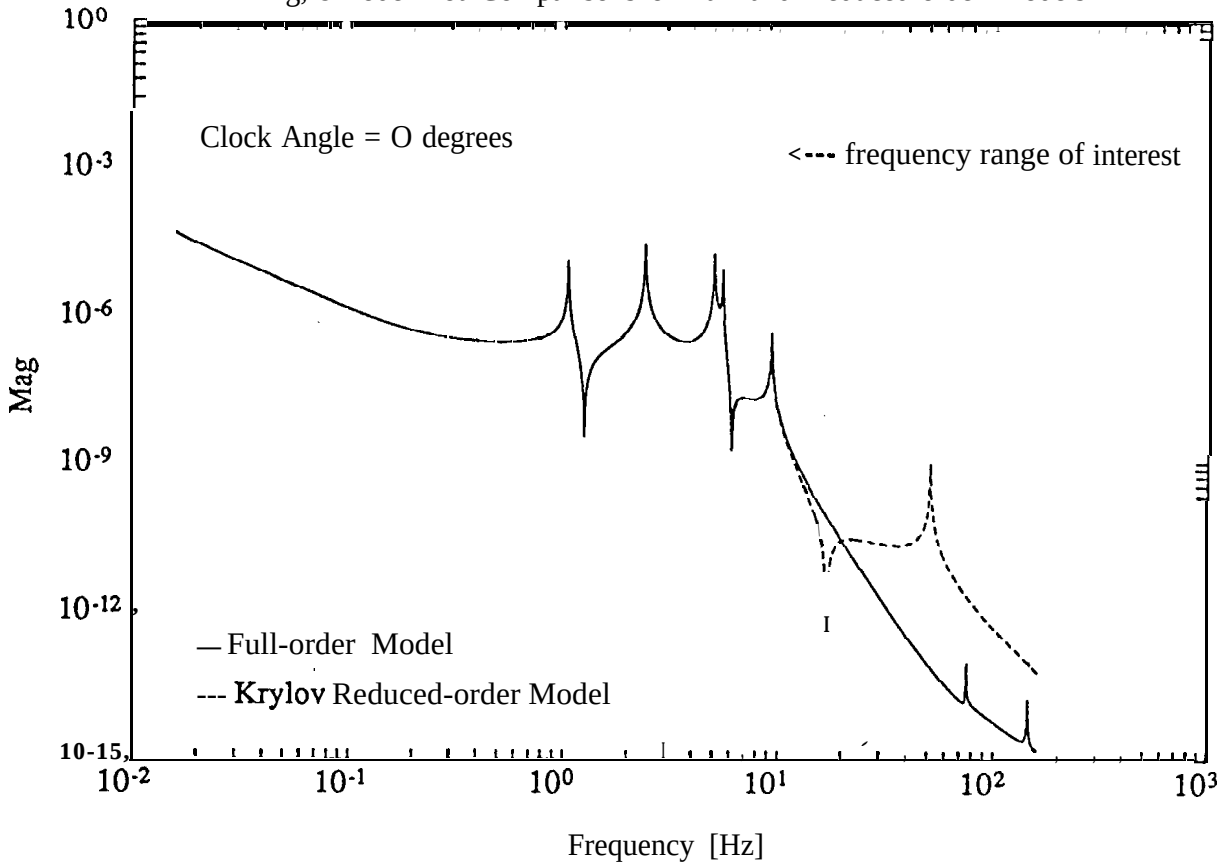

Figure 3 [Continued]

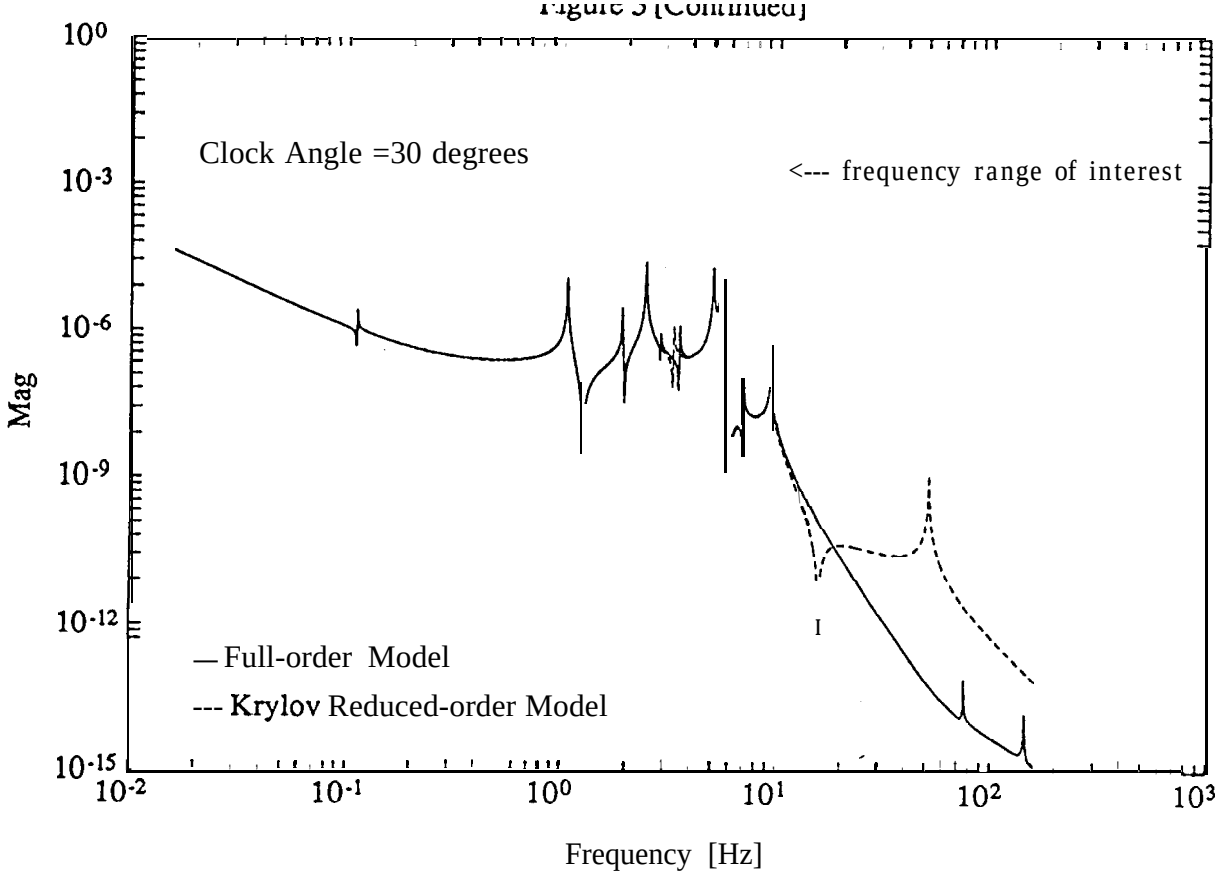

Figure 3 [Continued]

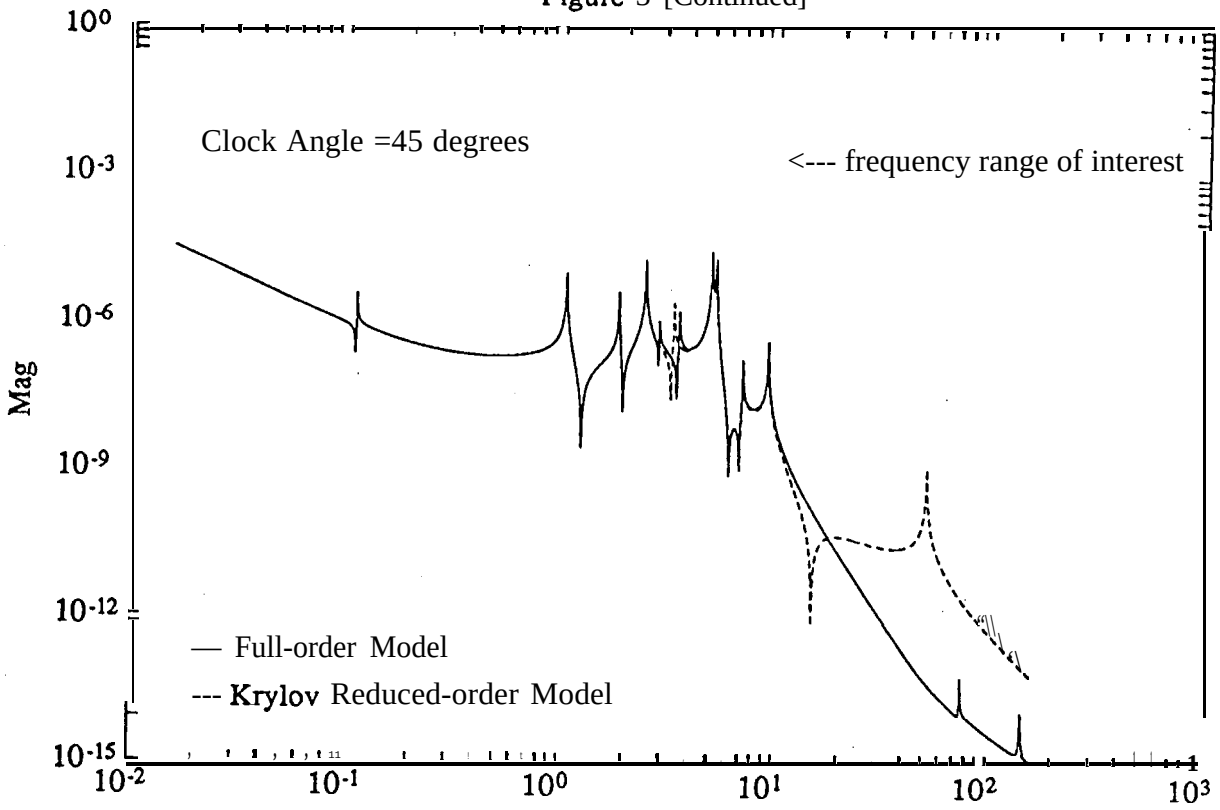

Figure 3 [Continued]